

1 **Skin Image Retrieval Using Gabor Wavelet Texture Feature**

2

3

4 **Abstract**

5 **OBJECTIVE:** Skin imaging plays a key role in many clinical studies. We have used
6 many skin imaging techniques, including the recently developed capacitive contact
7 skin imaging based on fingerprint sensors. The aim of this study is to develop an
8 effective skin image retrieval technique using Gabor wavelet transform, which can
9 be used on different types of skin images, but with a special focus on skin
10 capacitive contact images.

11

12 **METHODS:** Content-based image retrieval (CBIR) is a useful technology to retrieve
13 stored images from database by supplying query images. In a typical CBIR, images
14 are retrieved based on colour, shape, and texture, etc. In this paper, texture feature
15 is used for retrieving skin images, and Gabor wavelet transform is used for texture
16 feature description and extraction.

17

18 **RESULTS:** The results show that the Gabor wavelet texture features can work
19 efficiently on different types of skin images. Although Gabor wavelet transform is

20 slower comparing with other image retrieval techniques, such as Principal
21 Component Analysis (PCA) and Grey level co-occurrence matrix (GLCM), Gabor
22 wavelet transform is the best for retrieving skin capacitive contact images and facial
23 images with different orientations. Gabor wavelet transform can also work well on
24 facial images with different expressions and skin cancer/disease images.

25

26 **CONCLUSION:** We have developed an effective skin image retrieval method based
27 on Gabor wavelet transform, that it is useful for retrieving different types of images,
28 namely digital colour face images, digital colour skin cancer and skin disease
29 images, and grayscale skin capacitive contact images. Gabor wavelet transform
30 can also be potentially useful for face recognition (with different orientation and
31 expressions) and skin cancer/disease diagnosis.

32

33 **Keywords**

34 Skin imaging, skin capacitive images, content-based image retrieval, Gabor wavelet
35 transform, texture features.

36

37

38

39 **1. Introduction**

40 Skin imaging plays a key role in many research areas, such as dermatology, clinical
41 analysis, pharmacology and cosmetic science. In our previous research, we have
42 used many different imaging technologies, including standard digital camera,
43 DermLite Dermoscopy, Proscope HR and the recently developed capacitive contact
44 skin imaging based on fingerprint sensors [1-4]. As the number of skin images
45 soared, image retrieval became more and more important in our research. The aim
46 of this study is to develop an effective content-based image retrieving technique
47 that can work on different types of skin images, but with a particular focus on
48 grayscale capacitive contact skin images, where images are quite similar to each
49 other, and conventional image retrieving techniques normally do not work well.

50

51 Content-based image retrieval (CBIR), which is one of the popular fundamental
52 research in retrieving accurate useful information, is the set of techniques for
53 retrieving relevant images from an image database on the basis of image features
54 automatically extracted from an image database [5]. In the retrieval phase of a
55 CBIR system, the feature vector for each image in the database is calculated and
56 stored in feature database. After selecting a query image by the user, the matching
57 process that calculates the corresponding feature vector and compares it with all

58 the feature vectors related to the images in the database is performed. Images
59 having the minimum distance with the query image will be retrieved in a similarity
60 descending order [6,7]. In a typical CBIR, images are retrieved based on their visual
61 content such as colour, shape, and texture, etc. [8]. In this paper, texture feature is
62 used for retrieving images.

63

64 In image processing, texture which generally refers to the structures consisted of
65 large number of texture elements or models similar to each other, it is a key
66 component for human visual perception and plays an important role in
67 image-related applications. Meanwhile, texture features have been researched in
68 the content-based image retrieval, image classification and segmentation.
69 Gray-level co-occurrence matrix (GLCM) [9], Tamura texture feature [10], and
70 Gabor wavelet texture feature [11,12] are the conventional methods used to
71 describe texture feature. Compared with other techniques, Gabor wavelet texture
72 feature is much computationally simpler, and image analysis using Gabor wavelet
73 transform is similar to perception in the human visual system [13]. Gabor wavelet
74 transform has been used in optical character recognition, iris recognition and
75 fingerprint recognition. This paper describes a skin image retrieval technique based
76 on Gabor wavelet texture feature.

77

78 **2. Materials and Methods**79 2.1 Instruments

80 The main focus of this paper is capacitive contact skin images, but other images are
81 also used to test the performance of the algorithm. All the images used in this study
82 were taken by using standard digital camera and capacitance-based fingerprint
83 sensor, except the skin cancer and skin disease images, which were from Skin
84 Cancer page of About.com [21].

85

86 Standard digital camera used is SONY DSC--W55 model, which has a 7.2 Mega
87 Pixels with 3X optical zoom. Capacitance-based fingerprint sensor [2-4] is a novel
88 fringing field capacitive contact image technique that was developed in our research
89 group. It has a matrix of 256×300 pixels (capacitors) with $50 \mu\text{m}$ spatial resolution
90 per pixel. The total measurement area is $128 \times 15 \text{mm}^2$. The fingerprint sensor
91 basically generates a capacitance image of the skin surface. In each image, each
92 pixel is represented by an 8 bit grayscale value, 0~255, the higher grayscale values
93 mean the higher capacitances, and the lower grayscale values mean the lower
94 capacitances. Because in fringing field measurements, capacitance is determined
95 by the dielectric constants of the sample, and water has much higher dielectric

96 constants than dry skin, therefore, the higher capacitance means the higher water
97 content in skin, vice versa. Apart from water, the sensor is also sensitive to many
98 solvents that have relative high dielectric constant, such as dimethyl sulfoxide
99 (DMSO), ethylene glycol, propylene glycol, propanol, glycerol, and alcohol etc. [2].
100 This makes it a potentially a very useful tool for studying solvent penetrations
101 through membranes or skin, and trans-dermal drug delivery.

102

103 2.2 Gabor Wavelet Transform

104 Gabor wavelet can extract the relevant textural feature at different scales and
105 directions in the frequency domain and also has a good joint resolution in both
106 spatial and frequency domain [14]. Gabor wavelet is widely used to extract texture
107 features from the images for image retrieval and has been shown to be very
108 efficient [15-19].

109

110 The typical two dimensional Gabor function can be expressed as the production of
111 Gaussian function and sinusoidal function [19,20]:

112

$$113 \quad g(x,y) = \frac{1}{2\pi\sigma_x\sigma_y} e^{-\frac{1}{2}\left(\frac{x^2}{\sigma_x^2} + \frac{y^2}{\sigma_y^2}\right)} (e^{2\pi jfx}) \quad (1)$$

114

115 Where σ_x and σ_y are the Gaussian variance, which describe the spreads of the
 116 Gaussian function, j is the imaginary unit of complex number, f is the frequency of
 117 the sinusoidal function. Using Eq. 1 as the mother function, we can generate a set
 118 of child functions, called Gabor wavelets.

119

$$120 \quad g_m(x, y) = a^{-m} g(x', y') \quad a > 1, m, n = \text{integer}$$

$$121 \quad \begin{aligned} x' &= x \cos \theta + y \sin \theta \\ y' &= -x \sin \theta + y \cos \theta \end{aligned} \quad (2)$$

122

123 where $\theta = n\pi/K$, $n = 0, 1, \dots, K-1$, and K is the total number of the directions
 124 which specifies the orientation of a Gabor function; $m = 0, 1, \dots, S-1$, and S is the
 125 number of scales which specifies the amplitude of a Gabor function. If we use
 126 (U_l, U_h) to denote the lower and upper centre frequency of the sinusoidal function,
 127 we have

128

$$129 \quad \begin{aligned} a &= \frac{U_h}{U_l}^{\frac{1}{S-1}} \\ f &= U_h \end{aligned} \quad (3)$$

130

131 In this paper, the total number of directions (K) and scales (S) and have chosen to
132 be $K=6$ and $S=4$, respectively, which is resulting $4 \times 6=24$ Gabor wavelet
133 filters to filter the images. U_l and U_h used are 0.05 and 0.4, respectively.

134

135 Figure1 (A) shows typical profiles of Gaussian function, sinusoidal function and the
136 corresponding wavelet function; (B) shows the Gabor wavelet profiles at 6 different
137 directions and 4 different scales.

138

139 (Figure 1 goes in here)

140

141 Gabor wavelet transform can be considered as a wavelet transform whose mother
142 wavelet is Gabor function. For a given image $I(x, y)$ with $M \times N$ pixels, its Gabor
143 wavelet transform is defined as follows:

144

$$145 \quad W_m(x, y) = \int I(x_1, y_1) g_m^*(x - x_1, y - y_1) d_{x_1} d_{y_1} \quad (4)$$

146

147 where * represents the complex conjugate.

148

149

150 2.3 Experimental Procedures

151 A image database that includes 56 images in JPEG format was setup. Figure 2
152 shows some sample images from the database, which contains three different
153 types of images: human faces, skin cancer and skin disease images [21], and skin
154 grayscale capacitive contact images.

155

156 (Figure 2 goes in here)

157

158 A software programme has been developed to search above image database using
159 a query image, based the Gabor wavelet transform. A Graphic User Interface (GUI)
160 was also developed to simplify the operations. Following are the steps of the
161 programme:

- 162 1. Convert all the colour images into gray images.
- 163 2. Perform the Gabor wavelet transform on all images.
- 164 3. Calculate the mean and standard deviation as a texture feature.
- 165 4. Compare the texture feature of the query image with that of images in the
166 database, in order to find the best match results.

167

168

169 **3 Results and Discussions**

170 3.1 Image query results

171 Figure 3 shows the image retrieval results using Gabor texture features. In all the
172 four retrieval results shown, the best three retrieved images are shown for
173 illustration. The retrieved images are ranked in descending order according to the
174 similarity of their Gabor texture features to those of the query image, i.e. the most
175 similar, the second similar, and the third similar images. In this study, for simplicity
176 reasons, the query images are also from the database, and therefore the most
177 similar result should always be the image itself.

178

179 (Figure 3 goes in here)

180

181 In Figure 3(A), the query image is a grey capacitive image of finger skin, where
182 finger friction ridges are clearly visible. The black spots are the areas that water is
183 actively coming out of skin. As it can be seen, most of the best 3 retrieved images
184 are all similar finger grey capacitive images captured from Fingerprint sensor.
185 Figure 3(B) shows the retrieval results for a human face query image. Human face
186 images in the database are with two different expressions – smile and non-smile.
187 The most similar image is the same of query image. The second most similar image

188 is the same person without smile and the third image is that another person without
189 smile. It shows that this method has certain reference value for human face
190 recognition. It might be even also useful for facial expression recognition. Figure
191 3(C) and 3(D) are the output of skin cancer/disease retrieval results. The query
192 image in Figure 3(C) is a skin cancer image of melanoma. From the illustration, the
193 three of the most similar images are all skin cancer images. The query image in
194 Figure 3(D) is a skin disease image of leucoderma. From the results, the three of
195 the most similar images are all leucoderma images. The results show that Gabor
196 wavelet transform could also be potentially used for skin disease diagnostics. Users
197 could take a skin image, and search the skin disease database, and find out what
198 possible type of skin disease it might resemble, and seek doctors for early
199 diagnoses.

200

201 3.2 The effects of scales (S) and directions (K)

202 The values of scales (S) and directions (K) in Gabor wavelet transform not only
203 affect the accuracy of retrieval, they will also affect the computational time of
204 program. Figure 4(A) and 4(B) show typical retrieval errors when $S \times K = 2 \times 2$ and
205 Figure 4(C) shows the relationships between computational time and the production
206 of scales and directions ($S \times K$). If any of the best three results is not the right type of

207 images, such as Figure 4(A) or 4(B), we classify it as a retrieval error. Figure 4(C)
208 shows the relationships between retrieval errors and SxK. Generally speaking, the
209 higher the values of SxK, the lower the retrieval errors, but the longer the
210 computational time; the lower the values of SxK, the shorter the computational time,
211 but the higher the retrieval errors. The key is to find the optimum value of SxK that
212 has highest accuracy but lowest possible computational time. From this study, it is
213 found that setting scales and directions to 4 and 6 is a reasonable choice.

214 (Figure 4 goes in here)

215

216 3.3 The effects of U_l and U_h

217 Although the values of lower and higher centre frequency U_l and U_h do not affect
218 the computational time, they do effect the retrieval accuracy. In general, the values
219 of U_l and U_h are set to 0.05 and 0.4 because the lowest frequency of image is 0
220 and the highest frequency of image calculated from Nyquist sampling theorem is
221 0.5. According to the visual characteristics of the human eye, the frequency range
222 from 0.05 to 0.4 can be completely reflect people's perception of texture features
223 [22]. However, the retrieval results using these standard values shown in Figure 5
224 (A) are unsatisfactory because the query image in Figure 5 (A) is the neck grey
225 capacitive image, but the third most similar image is the face grey capacitive image.

226 By changing the value of U_l and U_h to 0.2 and 0.3 and the results shown in Figure
227 5 (B) become much better. From Figure 5, it can be concluded that the values of U_l
228 and U_h might need to be adjusted differently to different type of images in order to
229 have better retrieval accuracy.

230

231 (Figure 5 goes in here)

232

233

234 3.4 The performance of Gabor Wavelet Transform against other algorithms

235 In order to understand the performance of Gabor wavelet transform, we did an
236 image retrieval comparison study, compare Gabor wavelet transform against other
237 two algorithms: Principal Component Analysis (PCA) and Grey level co-occurrence
238 matrix (GLCM).

239

240 Table 1 shows the computation time of different algorithms. The results show that
241 GLCM is the fastest for calculating the feature vectors of all the images in the
242 database, whilst Gabor wavelet transform is the slowest. PCA is the fastest for
243 retrieving images, and Gabor wavelet transform is again the slowest.

244

245 **Table 1** The computation time used of each algorithm.

	PCA	GLCM	Gabor Wavelet Transform
Time 1	Average	Low	High
Time 2	Low	Average	High

246 Time 1: the time for calculating the feature vectors of all the images in the database.

247 Time 2: the time for retrieving the query image.

248

249 **Table 2** The retrieval success rates of each algorithm.

	PCA	GLCM	Gabor Wavelet Transform
Image type 1	Best	Worst	Average
Image type 2	Average	Worst	Best
Image type 3	Worst	Average	Best
Image type 4	Worst	Best	Average

250 Image type 1: human face images with different expressions.

251 Image type 2: human face images with different orientations.

252 Image type 3: grayscale capacitive skin images of different parts of human body.

253 Image type 4: skin diseases and skin cancer images.

254

255 Table 2 shows the successful retrieval rates of three different algorithms on different
256 type of skin images. Gabor wavelet transform is the best for retrieving capacitive
257 skin images and facial images with different orientations, GLCM is the best for
258 retrieving skin cancer / disease images, PCA is the best for retrieving facial images
259 with different expressions. The results also show that Gabor wavelet transform
260 works reasonably well for human faces with different expressions and skin cancer
261 and disease images.

262

263 **4 Conclusions and Future Works**

264 We have developed an effective skin image retrieval method based on Gabor
265 wavelet transform. Experimental results show that it is useful for retrieving different
266 types of images, namely digital colour face images, digital colour skin cancer and
267 skin disease images, and particularly suitable grayscale skin capacitive images.
268 The results also suggest that using the Gabor wavelets to extract texture features
269 could be useful for recognizing human face with different orientations and different
270 facial expressions, as well as for skin cancers and diseases diagnostics etc. In
271 Gabor wavelet transform, the values of scales, directions, lower and higher centre
272 frequency, might need to be adjusted differently according to different types of

273 images, in order to achieve a better retrieval results. For future work, we will
274 investigate to use another visual content such as colour and shape to retrieve
275 images.

276

277 **Acknowledgements**

278 We thank London South Bank University for the finance support of this project.

279

280 **References**

- 281 1. Singh, H., Development of a Measurement Instrument Using Capacitance
282 Sensors Techniques to Image and Measure the Skin Surface Hydration, PhD
283 Thesis, London South Bank University, November 2010.
- 284 2. Singh, H., Xiao, P., Berg, E.P., and Imhof, R.E., Skin Capacitance Imaging for
285 Surface Profiles and Dynamic Water Concentration Measurements, ISBS
286 Conference, Seoul, Korea, May 7-10, 2008.
- 287 3. Ou, X., Pan, W., Xiao, P., In vivo skin capacitive imaging analysis by using grey
288 level co-occurrence matrix (GLCM), International Journal of Pharmaceutics,
289 Available online 2 November 2013, ISSN 0378-5173,
290 <http://dx.doi.org/10.1016/j.ijpharm.2013.10.024>.
- 291 4. Xiao P., Ou X., Ciortea L.I., Berg E.P., Imhof R.E., In Vivo Skin Solvent
292 Penetration Measurements Using Opto-thermal Radiometry and Fingerprint
293 Sensor. Int J Thermophys. 33, 2012, 1787–1794.
- 294 5. Wang J.Z., Integrated Region-Based Image Retrieval. Boston:Kluwer Academic
295 2001, 1-5.
- 296 6. Rafiee, G., A review of content-based image retrieval. International Symposium
297 on Communication Systems Networks and Digital Signal Processing (CSNDSP),
298 2010,7, 775 - 779 .

- 299 7. Smeulders, A.W.M., Worring, M., Santini, S., Gupta, A., Jain, R., Content-Based
300 Image Retrieval at the End of the Early Years. IEEE TRANSACTIONS ON
301 PATTERN ANALYSIS AND MACHINE INTELLIGENCE. 22, 2000, 1349-1380.
- 302 8. Gong, Y., Zhang, H., Chuant, H. and Skauuchi. M., An image database system
303 with contents capturing and fast image indexing abilities. Proceedings of IEEE
304 International Conferences on Multimedia Computing and Systems,
305 Boston, Massachusetts, USA. 1994,5, 121–130.
- 306 9. Haralick, R.M., Shanmugam, K., and Dinstein. I., Texture features for image
307 classification. IEEETrans. Syst. Man Cybern. SMC(8), 1973,11, 610–621.
- 308 10. Hayes, K.C., Shah, Jr. A.N., and Rosenfeld, A., Texture coarseness: further
309 experiments. IEEETrans SMC-4, 467-472.
- 310 11. Yang, J., Liu, L., Jiang T., and Fan, Y., A modified Gabor filter design method
311 for fingerprint image enhancement. Pattern Recognition Letters. 24(12), 2003,
312 1805-1817.
- 313 12. Daugman, J.G., Uncertainty relation for resolution in space, spatial frequency,
314 and orientation optimized by twodimensional visual cortical filters. Journal of The
315 Optical Society of America. 2(7), 1985, 1160-1169.

- 316 13. Kruizinga, P., Petkov, N., and Grigorescu, S.E., Comparison of texture features
317 based on Gabor filters. Proceedings of the 10th International Conference on
318 Image Analysis and Processing. September 27-29, 1999, pp.142-147.
- 319 14. Smith, J.R., "Integrated Spatial and Feature Image System: Retrieval, Analysis
320 and Compression". Ph.D thesis, Columbia University, 1997.
- 321 15. Deng, Y., "A Region Representation for Image and Video Retrieval". Ph.D
322 thesis, University of California, Santa Barbara, 1999.
- 323 16. Dimai, A., Rotation Invariant Texture Description using General Moment
324 Invariants and Gabor Filters. Proc. Of the 11th Scandinavian Conf. on Image
325 Analysis. I, 1999, 6, 391-398.
- 326 17. Liu, Z, An Improved Face Recognition Method Based on Gabor Wavelet
327 Transform and SVM. Fifth International Symposium on Computational
328 Intelligence and Design (ISCID), 2012,10, 378 – 381.
- 329 18. Fischer, S., Minimum entropy transform using Gabor wavelets for image
330 compression. 11th International Conference on Image Analysis and Processing
331 and Proceedings, 2001,9,428 – 433.
- 332 19. Manjunath, B.S., and Ma, W.Y., Texture features for browsing and retrieval of
333 image data. IEEE Trans. Pattern Anal. Machine Intell. 18,1996,8, 837–842.

334 20. Skin cancer and skin diseases images,

335 http://skincancer.about.com/od/symptoms/ss/mole_all.htm

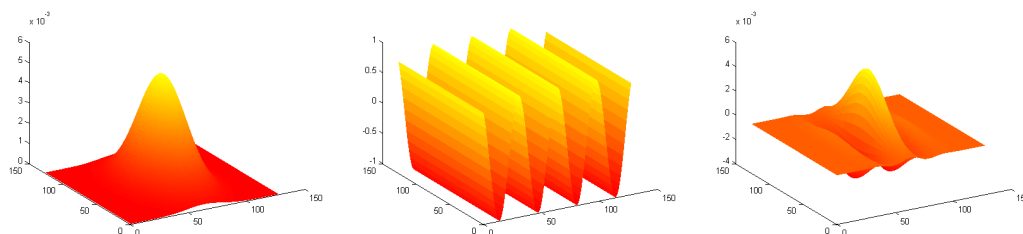
336 21. Anne H., Solberg S., Jain A.K. Texture fusion and feature selection applied to

337 SAR imagery [J]. IEEE transaction on Geoscience and Remote sensing. 35(2),

338 1997, 475-478.

339

340

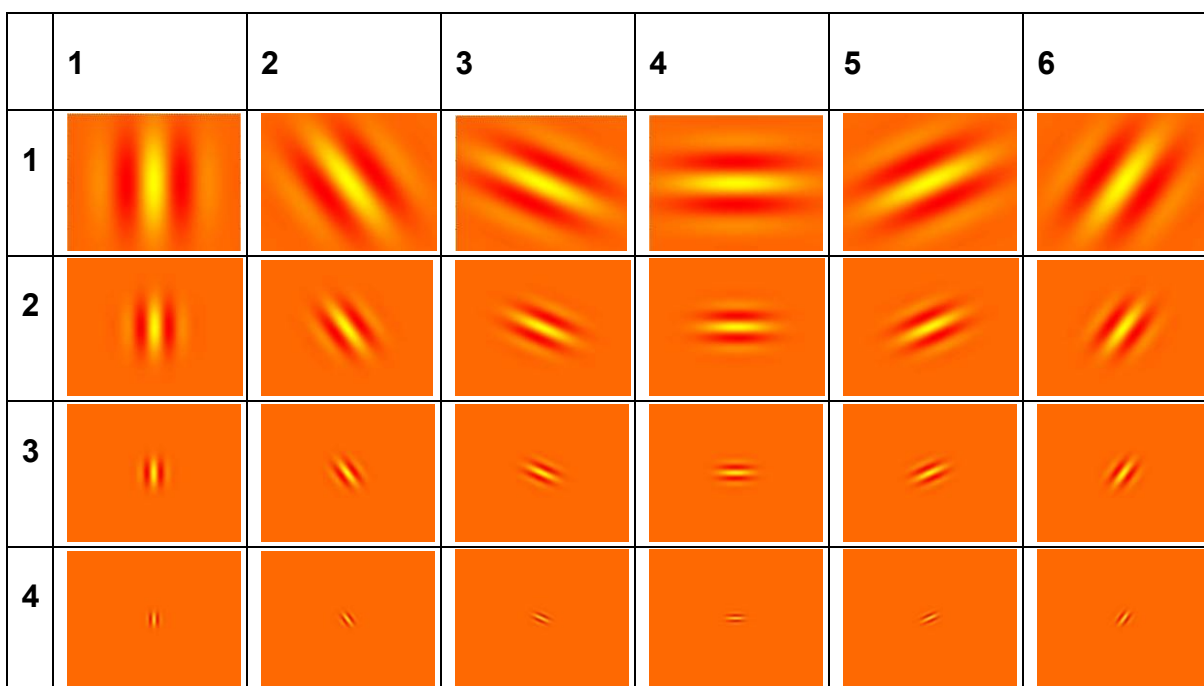


341

342

(A) Gaussian function Sinusoidal function Gabor function

343



344 (B) Top view of Gabor wavelet profiles at 6 different directions (columns) and 4

345 scales (rows).

346

347 **Figure 1.** Gabor wavelet profiles with at different directions and scales.

348

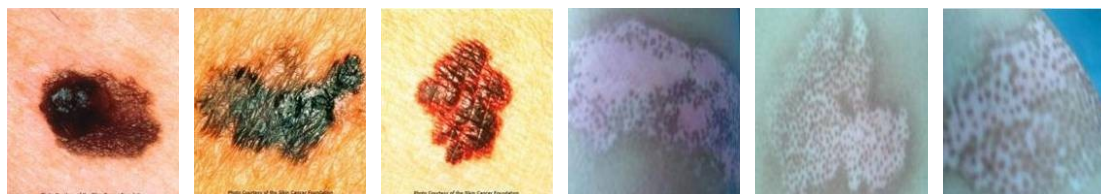
349



350

351

Faces

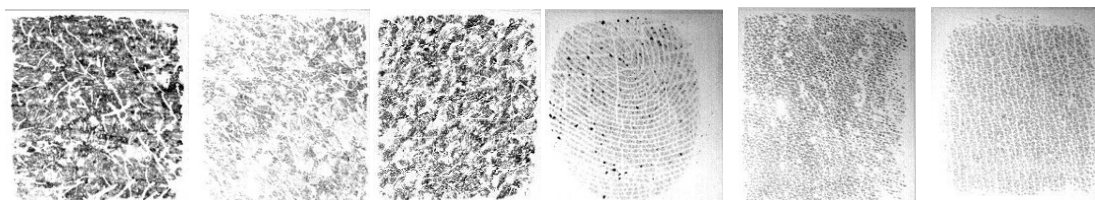


352

353

Skin cancers

Skin diseases



354

355

Capacitive skin images

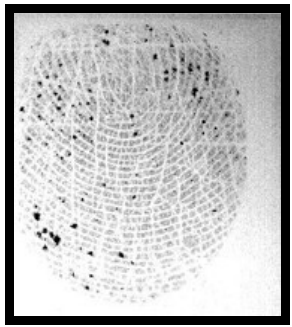
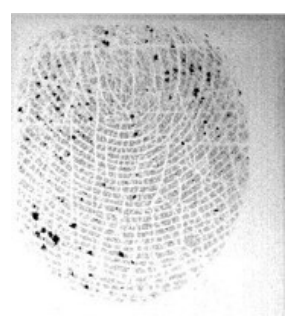
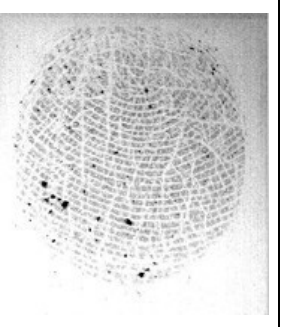
356

357 **Figure 2.** Sample images from the database.

358

359

(A)

Query Image	Search Results		
	Best	2nd	3rd
			

360

361

(B)

Query Image	Search Results		
	Best	2nd	3rd
			

362

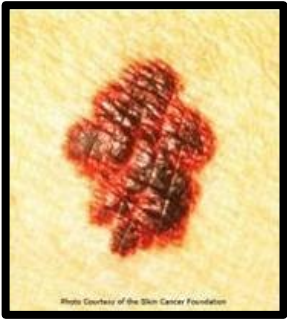
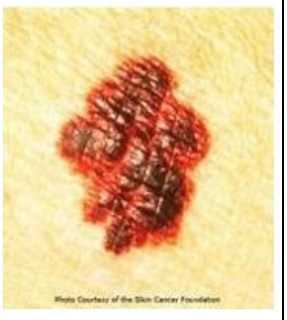
363

364

365

366

367 (C)

Query Image	Search Results		
	Best	2nd	3rd
			

368

369 (D)

Query Image	Search Results		
	Best	2nd	3rd
			

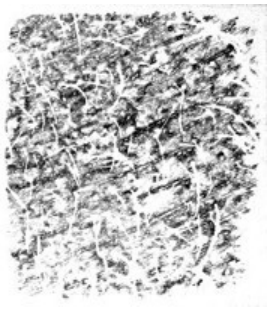
370

371 **Figure 3.** Image retrieval results using Gabor texture features.

372

373

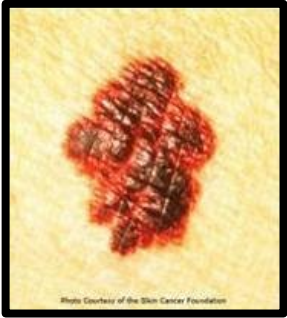
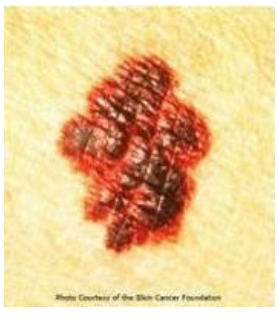
374 (A)

Query Image	Search Results		
	Best	2nd	3rd
			

375

376

377 (B)

Query Image	Search Results		
	Best	2nd	3rd
			

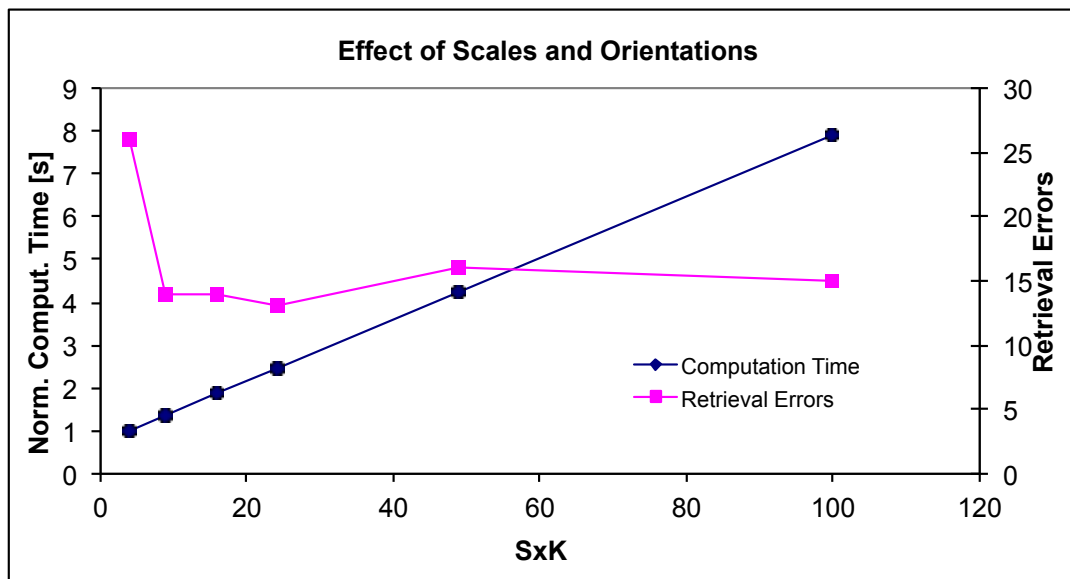
378

379

380

381

(C)



382

383

384

385 **Figure 4.** (A) and (B) are typical image retrieval errors when $SxK = 2x2$, (C) is

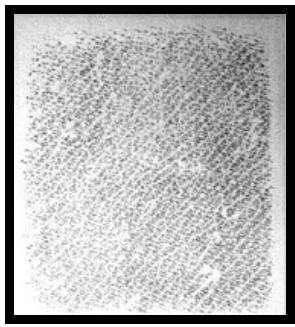
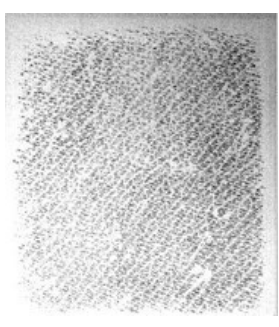
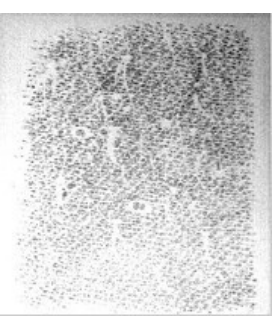
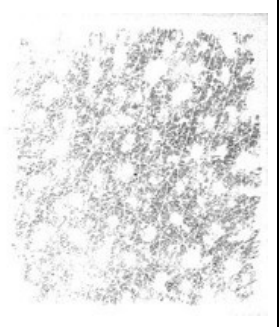
386 computational times and retrieval errors against the production of scales and

387 directions SxK .

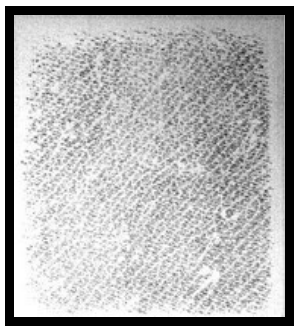
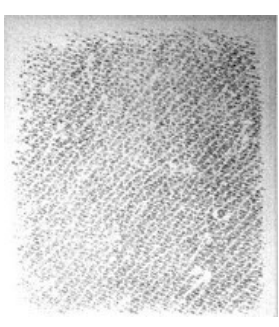
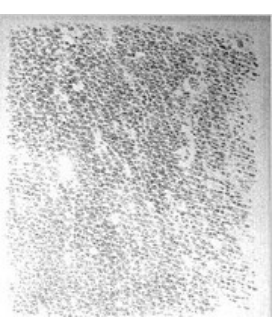
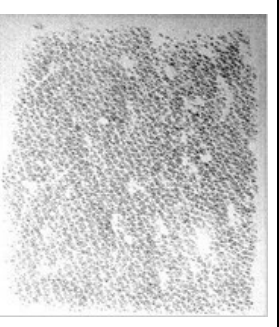
388

389

390 (A)

Query Image	Search Results		
	Best	2nd	3rd
			

391 (B)

Query Image	Search Results		
	Best	2nd	3rd
			

392

393

394 **Figure 5.** Image retrieval results using Gabor texture features when (A) $U_l = 0.05$

395 and $U_h = 0.4$ and (B) $U_l = 0.2$ and $U_h = 0.3$.

396